



## Abstract

New global maps of the depth to the boundary between the lithosphere and the asthenosphere are presented. The maps are based on updated global databases for heat flow and crustal structure. For continental regions the estimates of lithospheric thickness are based on determinations of subcrustal heat flow, after corrections for contributions of radiogenic heat in crustal layers. For oceanic regions the estimates of lithospheric thickness are based on the newly proposed finite half-space (FHS) model. Unlike the half-space cooling (HSC) and the Plate models the FHS model takes into account effects of buffered solidification at the lower boundary of the lithosphere and assumes that vertical domain for downward growth of boundary layer have an asymptotic limit. Results of numerical simulations reveal that theoretical values derived from FHS model provide vastly improved fits to observational data for heat flow and bathymetry than can be achieved with HSC and Plate models. Also, the data fits are valid for the entire age range of the oceanic lithosphere. Hence estimates of depths to lithosphere – asthenosphere boundary (LAB) based on FHS model, are believed to provide more reliable estimates than those reported in previous thermal models.

The global maps of depths to LAB derived in the present work reveal several features in regional variations of lithosphere thicknesses that have not been identified in earlier studies. For example, regions of ocean floor with ages less than 55Ma are characterized by relatively rapid thickening of the lithosphere. Also there is better resolution in mapping the transition from oceanic to continental lithosphere, as most of the latter ones are characterized by lithospheric thickness greater than 150 km. As expected the plate spreading centers in oceanic regions as well as areas of recent magmatic activity in continental regions are characterized by relatively thin lithosphere, with LAB depths of less than 50 km. On the other hand, the areas of continental collisions and Precambrian cratonic blocks and are found to have lithosphere thicknesses in excess of 250 km. Regional variations of lithosphere thickness in the interiors of continents are found to depend on the magnitude of subcrustal heat flux as well as the tectonic age of crustal blocks.

## Global distribution of the lithosphere-asthenosphere

V. M. Hamza and  
F. P. Vieira

Title Page

Abstract

Introduction

Conclusions

References

Tables

Figures



Back

Close

Full Screen / Esc

Printer-friendly Version

Interactive Discussion



## 1 Introduction

The concepts of lithosphere and asthenosphere are fundamental components of plate tectonic theory, according to which the lithosphere – asthenosphere boundary (LAB) separates the upper rigid part from the underlying upper mantle in both oceanic and continental regions. It is often considered as a first-order structural discontinuity that allows for differential motion between tectonic plates and the underlying mantle. Mapping the depth of LAB is important, since it is an essential constraint in models of formation and evolution of oceanic and continental regions. Detailed models of mantle convection depend on accurate knowledge of the depth variations of the LAB. In oceanic regions regional variations in heat flow and bathymetry has often been interpreted as indicative of systematic increase in the depth of LAB with distance from the spreading centers (for example: Parsons and Sclater, 1977). In continental areas thick lithospheric roots appear to exhibit large variations in thickness (Artemieva and Mooney, 2002; Eaton et al., 2009) and are likely to represent areas where the plates are strongly coupled to mantle flow (Conrad and Lithgow-Bertelloni, 2006). There are also evidences indicating that the lithosphere is thickest, strongest and most refractory within the cratonic nuclei of continents (e.g. Jordan, 1981; Praus et al., 1990).

Attempts to map LAB directly using seismological techniques have not had success, since the differential motion between lithosphere and asthenosphere is generally accommodated by passive deformation. Global observations of the Earth's gravity field show that the lithosphere is approximately in large-scale isostatic equilibrium (Sclater et al., 1975; Shapiro et al., 1999) and hence long-wavelength gravity inversion turns out to be an ineffective mapping tool. Results of magnetotelluric observations have, for many decades, been interpreted as indicative of an electrically conductive layer at depths beneath the continents consistent with seismic low velocity zones. Indirect methods have also been used in investigating the petrologic and geochemical characteristics of the LAB and adjacent regions. Nevertheless, there are considerable shortcomings in the methods employed in geologic studies and the results are plagued with large

SED

4, 279–313, 2012

### Global distribution of the lithosphere-asthenosphere

V. M. Hamza and  
F. P. Vieira

Title Page

Abstract

Introduction

Conclusions

References

Tables

Figures

⏪

⏩

◀

▶

Back

Close

Full Screen / Esc

Printer-friendly Version

Interactive Discussion



for the South American continent. At present the global data set consists of a total 41 386 heat flow measurements, of which 19 775 are in continental regions and 21 611 in oceanic regions. A summary of the data in continental and oceanic areas is provided in Table 1 and its global distribution illustrated in the map of Fig. 1.

This data set was employed in calculating mean heat flow for a regular grid system composed of  $1^\circ \times 1^\circ$  area elements. Such a grid system has a total of 63 800 cells, of which 22 380 are in continental areas and 42 420 are in oceanic areas. The results reveal that heat flow measurements have been carried out in areas corresponding to nearly 70 % of the grid cells. The remaining 30 % of the grid cells are devoid of observational data. Such inhomogeneous distributions of data are known to lead to problems in deriving global maps. One of the convenient techniques employed in overcoming such problems in data distribution is to make use of estimated values that are representative of the tectonic context. Following the practice adopted in the earlier works, we also have made use of the empirical predictor based on the well known heat flow – age relation in estimating values for cells devoid of experimental data. The heat flow values assigned for age provinces are based on a modified version of the results reported by Hamza (1967), Polyak and Smirnov (1968) and Hamza and Verma (1969). The modifications introduced takes into consideration advances obtained in determining the functional form of the relation between heat flow and age in North America, Australia, Europe, South America, Africa and Asia. The only exception is the region of Antarctica for which a constant heat flow value of  $45 \text{ m W m}^{-2}$  has been assigned.

The age values are derived from the geologic maps published by Mooney et al. (1998) for continental areas and Muller et al. (2008) for oceanic areas. Modern GIS (Geographic Information Science) techniques have been employed in deriving polygons that delimit sub units of geologic and structural provinces and the tectonic age pattern. These are superimposed on the reference grid system of  $1^\circ \times 1^\circ$  area elements which allowed determinations of the area segments of the geologic sub units and the values of mean heat loss for the corresponding “tectonic polygons”.

**Global distribution of  
the lithosphere-  
asthenosphere**V. M. Hamza and  
F. P. Vieira

Title Page

Abstract

Introduction

Conclusions

References

Tables

Figures

⏪

⏩

◀

▶

Back

Close

Full Screen / Esc

Printer-friendly Version

Interactive Discussion



## 2.2 Global heat flow maps

In calculating weighted mean values of heat flow for intersecting “tectonic polygons” we have assigned equal weights to both oceanic and continental data sets. Another outstanding feature of the present work concerns the use of heat flow data sets for ocean crust with ages less than 55 Ma. We have refrained from the practice (employed in some earlier works) of using theoretical heat flow values, derived from half-space cooling models, as substitutes for experimental data. The reason is the controversy concerning the hypothesis of regional scale hydrothermal circulation in young ocean crust. As pointed out by Hofmeister and Criss (2005) and Hamza et al. (2008) this hypothesis, which implies down flow of cold water in hot crust and up flow of hot water from cold crust, contradicts the basic principles of thermal convection in geologic media. In addition, the half space cooling models assume conductive heat loss from stagnant fluid bodies, a process unlikely to be representative of conditions in which lateral mass movements take place (Hamza et al., 2010).

The global heat flow map derived from the observational data set and estimated values are presented in Fig. 2. It reveals several features related to regional variations in both continental and oceanic regions. It is now possible to identify with much better resolution thermal anomalies associated with mid ocean ridges, areas of magmatic activity associated with subduction processes in back-arc regions and hot-spot localities in both oceanic and continental regions. Also, the map allows identification of areas of relatively low heat flow in the interiors of continents as distinct from areas of normal heat flow in continental platform areas and ocean basins.

## 3 Thermal models of the oceanic lithosphere: implications for LAB depths

The difficulties in mapping LAB depths in oceanic regions are in part related to fundamental problems in the thermal models of the lithosphere. For example, the so-called Half-Space Cooling (Turcotte and Oxburgh, 1967) and Plate models (McKenzie, 1967)

SED

4, 279–313, 2012

### Global distribution of the lithosphere-asthenosphere

V. M. Hamza and  
F. P. Vieira

Title Page

Abstract

Introduction

Conclusions

References

Tables

Figures

⏪

⏩

◀

▶

Back

Close

Full Screen / Esc

Printer-friendly Version

Interactive Discussion







### 3.3 FHS model

It is clear that we need to look for a model that accounts for the effects of latent heat of magma accretion and the process of buffered solidification at the base of the lithosphere. Hamza et al. (2010) presented a model that takes into consideration the thermal consequences of variable rates of magma accretion at the lower boundary of the lithosphere. According to this model (designated VBA) the variability in the rate of magma accretion at the base of the lithosphere has a direct influence on surface heat flux and bathymetry. More importantly, VBA model has been found to be capable of accounting for the main features in observational data sets of heat flow and bathymetry, without the need to invoke the hypothesis of regional scale hydrothermal circulation in ocean crust. Nevertheless, VBA model does not address explicitly the thermal effects of latent heat at the lithosphere – asthenosphere boundary.

Recently Cardoso and Hamza (2011) proposed a model that incorporate the effects of latent heat and buffered solidification and which at the same time provide a satisfactory solution for large scale variations of bathymetry and heat flux in the ocean floor. Designated as the Finite Half Space model – FHS, it introduces the assumption that the wavelength of the solution of the relevant heat conduction equation is related to the thickness of the stable lithosphere at large distances from the ridge axis. A major consequence of such a condition is that it imposes an asymptotic limit for the vertical growth of the lithosphere at the expense of the asthenosphere. Further, the FHS model assumes that solidification process is buffered, taking place between the liquidus and solidus temperatures ( $T_L$  and  $T_S$  respectively) of asthenospheric material at the base of the lithosphere. Under these conditions the solution for the temperature ( $T$ ) at depth ( $z$ ) in the oceanic lithosphere of age ( $t$ ) and of basal temperature ( $T_m$ ) is (Cardoso and Hamza, 2011):

$$T(z, t) = T_0 + (T_m - T_0) \frac{\operatorname{erf}\left(z / 2 \sqrt{\kappa_{\text{mod}} t}\right)}{\operatorname{erf}\left(a / 2 \sqrt{\kappa_{\text{mod}} t}\right)} \quad (3)$$

## Global distribution of the lithosphere-asthenosphere

V. M. Hamza and  
F. P. Vieira

Title Page

Abstract

Introduction

Conclusions

References

Tables

Figures

⏪

⏩

◀

▶

Back

Close

Full Screen / Esc

Printer-friendly Version

Interactive Discussion



where  $a$  is the asymptotic value for the thickness of the lithosphere in stable ocean basins and  $k_{\text{mod}}$  may be considered as the modified thermal diffusivity, that takes into account the role of latent heat:

$$\kappa_{\text{mod}} = \frac{\lambda}{\rho_{\text{Lit}}C_p - \rho_{\text{Ast}}L (dV/dT)} \quad (4)$$

5 In Eq. (4)  $\lambda$  is the thermal conductivity of the lithosphere,  $\rho_{\text{Ast}}$  and  $\rho_{\text{Lit}}$  the densities of asthenosphere and lithosphere respectively and  $L$  the latent heat of solidification of the asthenospheric material at the base of the lithosphere. The expression  $dV/dT$  in Eq. (4) is the volumetric proportion of the solidification reaction assumed to be buffered between the liquidus ( $T_L$ ) and solidus ( $T_S$ ) temperatures. For unit change in temperature  
10 the variation of  $V$  is defined as:

$$V(T) = \frac{(e^{bT} - e^{bT_S})}{(e^{bT_L} - e^{bT_S})} \quad (5)$$

In Eq. (5)  $b$  is a constant that determines partitioning between the liquid and solid fractions in the buffered solidification process. Note that  $V$  in Eq. (5) has the unit of percent and not cubic meters.

15 A careful examination of the Eq. (3) reveal that the solution provided by the FHS model represents in fact the general case and the solutions derived in the HSC and Plate models are particular end member cases. This can easily be verified by noting that for small values of time ( $t$ ) and values of depth ( $z$ ), much less than the thickness of the stable lithosphere ( $a$ ), the right hand side of Eq. (1) is nearly identical to that of the  
20 fundamental solution for temperature in the HSC model, the only difference being the modified form of thermal diffusivity. On the other hand, for depth values ( $z$ ) nearly equal to the stable thickness of the lithosphere ( $a$ ) the right hand side of Eq. (1) approaches unity, which is the condition employed in the Plate model of McKenzie (1967). In other words, the FHS model behavior is similar to that of the HSC model for small times but  
25 similar to that of the Plate model for larges times.

**Global distribution of the lithosphere-asthenosphere**

V. M. Hamza and  
F. P. Vieira

Title Page

Abstract

Introduction

Conclusions

References

Tables

Figures

⏪

⏩

◀

▶

Back

Close

Full Screen / Esc

Printer-friendly Version

Interactive Discussion



The equation for surface heat flux obtained from Eq. (1) by Cardoso and Hamza (2011) is:

$$q(t)_{z=0} = \lambda \frac{(T_m - T_0)}{\sqrt{(\pi \kappa_{\text{mod}} t)}} \frac{1}{\text{erf}\left(a/2\sqrt{\kappa_{\text{mod}} t}\right)} \quad (6)$$

Cardoso and Hamza (2011) also developed the following relation for bathymetry in FHS model, following the isostatic compensation scheme discussed in earlier studies (e.g. McKenzie, 1967; Sclater and Francheteau, 1970; Parsons and Sclater, 1977):

$$e(t) = d_r + \frac{\alpha a T_m \rho_a}{\sqrt{\pi}(\rho_a - \rho_w)} \left[ \frac{1 - e^{-\left(a/2\sqrt{\kappa_{\text{mod}} t}\right)^2}}{\left(a/2\sqrt{\kappa_{\text{mod}} t}\right) \text{erf}\left(a/2\sqrt{\kappa_{\text{mod}} t}\right)} \right] \quad (7)$$

The fits to the observational data sets for heat flow and ocean floor bathymetry, on the basis of Eqs. (6) and (7), are presented respectively in the upper and lower panels of Fig. 3. Also illustrated in this figure are the fits provided by the GDH model of Stein and Stein (1992). It is fairly simple to note that the fit of FHS model to observational heat flow data is far superior to that which can be produced by HSC, GDH and Plate models. More importantly, the fits obtained are valid for the entire age range of the oceanic lithosphere, there being no need to invoke the hypothesis of regional scale hydrothermal circulation in ocean crust. In the case of bathymetry GDH and FHS model fits are almost identical. Nevertheless, the GDH model fit requires the hybrid scheme, with changes in bathymetry calculations at the age value of 25Ma for the ocean crust.

### 3.4 LAB depths

We now examine the fit of FHS model to oceanic heat flow data as part of the attempt to map regional variations in the depth of LAB in oceanic regions. In this task it is important to set a value for basal temperature that is compatible with results of petrology and

## Global distribution of the lithosphere-asthenosphere

V. M. Hamza and  
F. P. Vieira

Title Page

Abstract

Introduction

Conclusions

References

Tables

Figures

⏪

⏩

◀

▶

Back

Close

Full Screen / Esc

Printer-friendly Version

Interactive Discussion



thermal models of the lithosphere. However, there is no universal agreement as to the representative value of the basal temperature to be used in model studies of the lithosphere. According to Green et al. (2001) primary magmas in the Hawaiian region have an average temperature of 1365 °C, but presence of even small amounts of volatiles can lead to temperatures as low as 1000 °C. McKenzie and Bickl (1988) infer that asthenosphere have a potential temperature of 1280 °C. McNutt (1990) and Jaupart and Mareschal (1999) assume that the thickness of the mechanical lithosphere is proportional to the thickness of the conductive thermal boundary layer and defines the base of the thermal lithosphere as the intersection of the geotherm with the mantle adiabat of 1300 °C. Parsons and Sclater (1977) and Sclater et al. (1980) used observational data on bathymetry of various oceans to estimate the best fitting value of 1333 °C for the basal temperature. The same approach was used by Stein and Stein (1992) who argued that a basal temperature of 1450 °C at a depth of 95 km fit the data better than the values estimated by Parsons and Sclater (1977). For purposes of the present work the basal temperature of lithosphere is assumed to fall in the interval of 1250 to 1350 °C. The time variation of LAB for oceanic lithosphere, derived from Eq. (3), is illustrated in Fig. 4.

Figure 5 provides a comparison of the thickness variations of the lithosphere according to the Finite Half Space (FHS) and Half-Space Cooling (HSC) models. The dashed curves in this figure indicate depths of LAB derived from the HSC model, which plunge to values of more than 90 km, for ages greater than 55 Ma. On the other hand, the FHS model depths to LAB approach asymptotic values of no more than 90 km for age values in excess of 80 Ma. This asymptotic limit is compatible with the thickness of the stable lithosphere in ocean basins. Another remarkable feature of FHS model is that regions of ocean floor with ages less than 25 Ma are characterized by relatively rapid thickening of the lithosphere, when compared with the HSC model values. This is also a consequence of the FHS model, which imposes a rapid decrease in magma accretion rates at the base of the lithosphere, as it moves away from the ridge axis. The most important conclusion is that the depth to LAB of oceanic lithosphere is controlled

## Global distribution of the lithosphere-asthenosphere

V. M. Hamza and  
F. P. Vieira

[Title Page](#)[Abstract](#)[Introduction](#)[Conclusions](#)[References](#)[Tables](#)[Figures](#)[⏪](#)[⏩](#)[◀](#)[▶](#)[Back](#)[Close](#)[Full Screen / Esc](#)[Printer-friendly Version](#)[Interactive Discussion](#)





## Global distribution of the lithosphere-asthenosphere

V. M. Hamza and  
F. P. Vieira

Title Page

Abstract

Introduction

Conclusions

References

Tables

Figures

⏪

⏩

◀

▶

Back

Close

Full Screen / Esc

Printer-friendly Version

Interactive Discussion

employed in determining mean crustal thickness and mean velocity values for a regular grid system of  $2^\circ \times 2^\circ$  cells. Calculations carried out for this system of cells has allowed determination of regional variations of crustal heat production values in continental and oceanic regions. The results are employed in calculating the heat flux produced by radioactive elements in the crust. The map of Fig. 8 illustrates the global distribution of radiogenic heat flux. As expected contribution of radiogenic heat production is significant mainly in areas of continental crust. Oceanic crust is practically free of any significant quantities of radiogenic heat.

### 4.3 Thermal model of continental crust

The temperature in the continental lithosphere can be approximated by the steady state solution of the one dimensional heat conduction equation. For a medium with depth dependant thermal conductivity ( $\lambda$ ) and exponential decrease of heat production ( $A$ ) in the vertical direction ( $z$ ) the solution for temperature ( $T$ ) may be expressed as (Hamza, 1982):

$$(\lambda_0/\alpha) \ln(u/u_0) = (q_0 - A_0 D)z + A_0 D^2 \left[ 1 - e^{-z/D} \right] \quad (9)$$

where  $u = 1 + \alpha T$ ,  $\alpha$  being the temperature coefficient of thermal conductivity and  $D$  is the logarithmic decrease in heat production with depth. The terms with subscripts zero ( $\lambda_0$ ,  $q_0$  and  $A_0$ ) represent values of the parameters (thermal conductivity, heat flux and radiogenic heat production, respectively) at the surface ( $z = 0$ ).

### 4.4 Mantle heat flow

The procedure outlined in the previous section has been employed in the present work for determining vertical variations in heat flux for the  $2^\circ \times 2^\circ$  grid system. This work is greatly facilitated by updated global databases for heat flow (Vieira and Hamza, 2010) and crustal structure (Mooney et al., 1998). Heat flow values corrected for contributions of radiogenic heat were calculated at depths corresponding to the base of sedimentary

strata, the upper crust and the lower crust. Note that the basal heat flux for the lower crust is the same as the mantle heat flux.

Equation (6) permits calculation of temperatures, constrained primarily by surface heat flow measurements and the vertical distribution of thermal parameters (thermal conductivity and heat production), within the crust and in the lithospheric mantle. It also allows determinations of vertical heat flux at any depth level in the crust. In other words, we have a means of implementing a back-stripping process for determining deep heat flux with progressive elimination of the contributions radiogenic heat in overlying layers. The results obtained in such a back-stripping process are illustrated in the set of maps of Fig. 9. The upper panel in this figure indicates global distribution of heat flow at the base of sedimentary layer, which is nearly the same as surface heat flow. It is clear that near surface heat flow provides very little clues as to the contrasts in the deep thermal structures of continental and oceanic regions. The middle and lower panels of Fig. 9 refer respectively to the cases where the contributions of radiogenic heat of the upper and lower crust are removed by the back-stripping processes. It is clear that progressive removal of the contributions of radiogenic heat of upper and lower crustal layers bring into evidence the differences in deep heat flux. A remarkable feature in the middle panel of Fig. 9 is the relatively narrow width of the transition zone of deep heat flux, between continental and oceanic regions. It is a clear indication that the heat producing sources are situated at shallow depths in the crust. Another outstanding feature, evident in the lower panel of this figure, is the contrast in the global distribution of mantle heat flux, which is less than  $40 \text{ m W m}^{-2}$  in most areas of continental crust.

## 5 Global distribution of LAB depths

We now examine the global distribution of depths to LAB based on the results discussed in the previous Sects. 3 and 4. As in the case of oceanic regions it is important to set a value for basal temperature that is compatible with studies of petrology and thermal models of the continental lithosphere. Again, there is no universal agreement

SED

4, 279–313, 2012

## Global distribution of the lithosphere-asthenosphere

V. M. Hamza and  
F. P. Vieira

Title Page

Abstract

Introduction

Conclusions

References

Tables

Figures

⏪

⏩

◀

▶

Back

Close

Full Screen / Esc

Printer-friendly Version

Interactive Discussion



as to the representative value of the basal temperature to be used in model studies of the continental lithosphere.

In continental regions estimates of basal temperatures of periods extending back to Archean times have been made based on analysis of mantle xenoliths. For example,  $P - T$  conditions inferred for xenoliths from Northern Lesotho is 1050 to 1250 °C at depths of 170 km (O'Reilly and Griffin, 2006; Grütter et al., 2006). The xenolith data for the Slave Province in Canada reported by Kopylova et al. (1999) indicate that the conductive geotherm in the mantle extrapolates to the mantle adiabat with temperatures of 1350 °C at depths of 200 km. Though there are considerable uncertainties in the methodology it is fairly reasonable to conclude that the xenolith geotherms serve as upper limits for present day basal temperatures of the continental lithosphere. Thus a mantle adiabat of 1300 °C is considered as representative of the Precambrian cratons. However, as mantle convection depends on viscosity, which is itself temperature dependent, the base of the thermal lithosphere is sometimes defined as 0.85 times the solidus temperature. In this case basal temperatures would be somewhat lower, around 1100 °C for a mantle solidus of 1300 °C (Pollack and Chapman, 1977). For purposes of the present work the basal temperature of lithosphere is assumed to fall in the interval of 1100 to 1300 °C.

As in the case of heat flow and radiogenic heat production data sets (discussed in Sects. 2 and 4, respectively) a regular grid system of 2° × 2° cells was used in calculating mean values of depths to LAB. The data set generated in this procedure was used in deriving maps of the global distribution of LAB depths. One of the convenient forms of representing such gridded data sets is through the technique of spherical harmonic representation. The main limitation of this technique is the elimination of short wavelength variations resulting in loss of resolution. An alternative is to make use of the numerical interpolation schemes which may be coupled with automatic contouring techniques. The maps of global distribution of LAB depths derived these two approaches are presented in the two panels of Fig. 10. In this figure, the upper panel refers to the map produced by spherical harmonic representation while the lower panel

## Global distribution of the lithosphere-asthenosphere

V. M. Hamza and  
F. P. Vieira

[Title Page](#)[Abstract](#)[Introduction](#)[Conclusions](#)[References](#)[Tables](#)[Figures](#)[Back](#)[Close](#)[Full Screen / Esc](#)[Printer-friendly Version](#)[Interactive Discussion](#)

refers to the map by numerical interpolation. The maps obtained in both types of representations reveal that LAB depths are less than 50 km in areas of sea floor spreading. Examples are the approximately north – south trending mid-ocean ridge systems in the Atlantic, Pacific and Indian Ocean areas. Other regions of relatively thin lithosphere are the back-arc regions associated with subduction zones. In continental regions Cenozoic rift zones and areas of recent magmatic activity stand out as areas of shallow LAB.

On the other hand, the interior parts of continental regions are characterized by thick lithosphere. The Archean cratons with relatively thick lithospheric roots includes Siberian Platform, West Africa, Baltic Shield, South Africa, Western Australia, the Indian Shield, Cathaysian Craton, and the Sao Francisco Craton in South America. There are some indications of progressive thickening of the lithosphere in areas of cratonic nuclei.

## 6 Discussion and conclusions

The present work has allowed derivation of new global maps of the depth to the boundary between the lithosphere and the asthenosphere. The maps are based on updated global databases for heat flow (Vieira and Hamza, 2010) and crustal structure (Mooney et al., 1998). For continental regions the estimates of lithospheric thickness are based on determinations of subcrustal heat flow, after corrections for contributions of radiogenic heat in crustal layers. For oceanic regions the estimates of lithospheric thickness are based on the newly proposed finite half-space (FHS) model. Results of numerical simulations reveal that theoretical values derived from FHS model provide vastly improved fits to observational data for heat flow and bathymetry than can be achieved with HSC and Plate models. Hence estimates of depths to lithosphere – asthenosphere boundary (LAB) based on FHS model, are believed to provide more reliable estimates than those reported in previous thermal models.

The global maps of depths to LAB derived in the present work reveal several features in regional variations of lithosphere thicknesses that have not been identified in earlier

SED

4, 279–313, 2012

## Global distribution of the lithosphere-asthenosphere

V. M. Hamza and  
F. P. Vieira

Title Page

Abstract

Introduction

Conclusions

References

Tables

Figures

⏪

⏩

◀

▶

Back

Close

Full Screen / Esc

Printer-friendly Version

Interactive Discussion





*Acknowledgements.* This work was carried out as part of research project with funding from Conselho Nacional de Desenvolvimento Científico – CNPq (Project No. 301865/2008-6; Produtividade de Pesquisa – PQ). Thanks are due to Andres Papa (ON- Observatório Nacional) for institutional support.

## 5 References

- Artemieva, I. M.: Global  $1^\circ \times 1^\circ$  thermal model TC1 for the continental lithosphere: Implications for lithosphere secular evolution, *Tectonophysics*, 416, 245–277, 2006.
- Artemieva, I. M. and Mooney, W. D.: Thermal thickness and evolution of Precambrian lithosphere: A global study, *J. Geophys. Res.*, 106, 16387–16414, 2001.
- 10 Artemieva, I. M. and Mooney, W. D.: On the relations between cratonic lithosphere thickness, plate motions, and basal drag, *Tectonophysics*, 358, 211–231, 2002.
- Bassin, C., Laske, G., and Masters, G.: The current limits of resolution for surface wave tomography in North America, *EOS Trans. AGU*, 81, 897, 2000.
- Cardoso, R. R. and Hamza, V. M.: Crustal heat flow variations of in the Equatorial Atlantic: implications for geothermal structure of NE Brazil, in: *Proceedings of the 2nd symposium of the Brazilian Geophysical Society, Natal*, 6 pp., 2006.
- 15 Cardoso, R. R. and Hamza, V. M.: A Simple conduction advection model of the lithosphere and possible demise of the hypothesis of regional hydrothermal circulation in the ocean crust, in: *Proceedings of the 10th Int. Congress of the Brazilian Geophys. Society, Rio de Janeiro, Brazil*, 2007.
- Cardoso, R. R. and Hamza, V. M.: Finite Half-Space Model of Oceanic Lithosphere, in: *Horizons in Earth Science Research*, edited by: Veress, B. and Szegedy, J., 11, 375–395, 2011.
- Carlsaw, H. S. and Jaeger, J. C.: *Conduction of Heat in Solids*, Oxford University Press, New York, NY, USA, 2nd Edition, 1959.
- 25 Cermak, V. and Bodri, L.: A heat production model of the crust and upper mantle, *Tectonophysics*, 194, 307–323, 1991.
- Conrad, C. P. and Lithgow-Bertelloni, C.: Influence of continental roots and asthenosphere on plate-mantle coupling, *Geophys. Res. Lett.*, 33, L05312 doi:10.1029/2005GL025621, 2006.
- Cull, J. P.: Heat Flow and Regional Geophysics in Australia, in: *Terrestrial Heat Flow and the*

SED

4, 279–313, 2012

## Global distribution of the lithosphere-asthenosphere

V. M. Hamza and  
F. P. Vieira

Title Page

Abstract

Introduction

Conclusions

References

Tables

Figures

◀

▶

◀

▶

Back

Close

Full Screen / Esc

Printer-friendly Version

Interactive Discussion

## Global distribution of the lithosphere-asthenosphere

V. M. Hamza and  
F. P. Vieira

Title Page

Abstract

Introduction

Conclusions

References

Tables

Figures

⏪

⏩

◀

▶

Back

Close

Full Screen / Esc

Printer-friendly Version

Interactive Discussion



Lithosphere Structure, edited by: Cermak, V. and Rybach, L., Springer, New York, 486–500, 1991.

Davies, J. H. and Davies, D. R.: Earth's surface heat flux, *Solid Earth*, 1, 5–24, doi:10.5194/se-1-5-2010, 2010.

5 Eaton, D. W., Darbyshire, F., Evans, R. L., Grütter, H., Jones, A. G., and Yuan, X.: The elusive lithosphere-asthenosphere boundary (LAB) beneath cratons, *Lithos*, 109, 1–22, 2009.

Fischer, K. M., Ford, H. A., Abt, D. L., and Rychert, C. A.: The Lithosphere-Asthenosphere Boundary, *Annu. Rev. Earth Planet. Sci.*, 38, 551–575, 2010.

Green, D. H., Falloon, T. J., Eggins, S. M., and Yaxley, G. M.: Primary magmas and mantle temperatures, *Eur. J. Mineral*, 13, 437–451, 2001.

10 Grütter, H., Latti, D., and Menzies, A.: Cr-saturation arrays in concentrate garnet compositions from Kimberlite and their use in mantle barometry, *J. Petrol.*, 47, 801–820, 2006.

Hamza, V. M.: The relationship of heat flow with geologic age, Internal Report, National Geophysical Res. Institute, Hyderabad (India), 1967.

15 Hamza, V. M.: Thermal Structure of South American Continental Lithosphere During and Proterozoic, *Rev. Bras. Geociências*, São Paulo, Brazil, 149–159, 1982.

Hamza, V. M. and Verma, R. K.: Relationship of heat flow with the age of basement rocks, *Bull. Volcan.*, 33, 123–152, 1969.

Hamza, V. M., Cardoso, R. R., and Ponte Neto, C. F.: Global Heat flow: Fantasy and Facts (Abstract), Sixth International Meeting Heat Flow and the Structure of the Lithosphere, Bykov (Czech Republic), 47 pp., 2006.

Hamza, V. M., Cardoso, R. R., and Ponte Neto, C. F.: Spherical Harmonic Analysis of Earth's Conductive Heat Flow, *Int. J. Earth Sci.*, 97, 205–226, 2008a.

Hamza, V. M., Cardoso, R. R., and Ponte Neto, C. F.: Reply to Comments by Henry, N. Pollack and David, S. Chapman on "Spherical Harmonic Analysis of Earth's Conductive Heat Flow", *Int. J. Earth Sci.*, 97, 233–239, 2008b.

Hamza, V. M., Cardoso, R. R., and Alexandrino, C. H.: A Magma Accretion Model for the Formation of Oceanic Lithosphere: Implications for Global Heat Loss, *Int. J. Geophys.*, 2010, 146496, 16 pp., doi:10.1155/2010/146496, 2010.

30 Hofmeister A. M. and Criss R. E.: Earth's heat flux revised and linked to chemistry, *Tectonophysics*, 395, 159–177, 2005.

Iyer, S. S., Babinski, M., and Hamza, V. M.: Radiogenic heat production in sedimentary rocks of the Bambui Group: Implications for thermal history and hydrocarbon generation, *Proceed-*



## Global distribution of the lithosphere-asthenosphere

V. M. Hamza and  
F. P. Vieira

Title Page

Abstract

Introduction

Conclusions

References

Tables

Figures

⏪

⏩

◀

▶

Back

Close

Full Screen / Esc

Printer-friendly Version

Interactive Discussion



- Praus, O., Pecova, J., Petr, V., Babuska, V., and Plomerova, J.: Magnetotelluric and seismological determination of the lithosphere-asthenosphere transition in Central Europe, *Phys. Earth Planet. In.*, 60, 212–228, 1990.
- Rybach, L. and Buntebarth, G.: The variation of heat generation, density and seismic velocity with rock type in the continental lithosphere, in: *Terrestrial Heat Flow Studies and the Structure of the Lithosphere*, edited by: Cermak, V., Rybach, L., and Chapman, D. S., *Tectonophysics*, 103, 335–344, 1984.
- 5 Sclater, J. G. and Francheteau, J.: The implications of terrestrial heat flow observations on current tectonic and geochemical models of the crust and upper mantle of the Earth, *Geophys. J. Roy. Astr. Soc.*, 20, 509–542, 1970.
- 10 Sclater, J. G., Lawver, L. A., and Parsons, B.: Comparison of Long-Wavelength Residual Elevation and Free-Air Gravity Anomalies in the North Atlantic and Possible Implications for the Thickness of the Lithospheric Plate, *J. Geophys. Res.*, 80, 1031–1052, 1975.
- 15 Sclater, J. G., Jaupart, C., and Galson, D.: The heat flow through oceanic and continental crust and the heat loss of the Earth, *Rev. Geophys.*, 18, 269–311, 1980.
- Shapiro, S. S., Hager, B. H., and Jordan, T. H.: The continental tectosphere and Earth's long-wavelength gravity field, *Lithos*, 48, 135–152, 1999.
- Smithson, S. B. and Decker, E. R.: A continental crustal model and its geothermal implications, *Earth Planet. Sci. Len.*, 22, 215–225, 1974.
- 20 Stein, C. and Stein, S.: A model for the global variation in oceanic depth and heat flow with lithospheric age, *Nature*, 359, 123–129, 1992.
- Turcotte, D. L. and Oxburgh, E. R.: Finite amplitude convective cells and continental drift, *The J. Fluid Mechanics*, 28, 29–42, 1967.
- 25 Vieira, F. P. and Hamza, V. M.: Global Heat Loss: New Estimates Using Digital Geophysical Maps and GIS Techniques, *Proceedings of the IV Symposium of the Brazilian Geophysical Society*, 14–17 November 2010, 1–6, 2010.

## Global distribution of the lithosphere-asthenosphere

V. M. Hamza and  
F. P. Vieira

Title Page

Abstract

Introduction

Conclusions

References

Tables

Figures

⏪

⏩

◀

▶

Back

Close

Full Screen / Esc

Printer-friendly Version

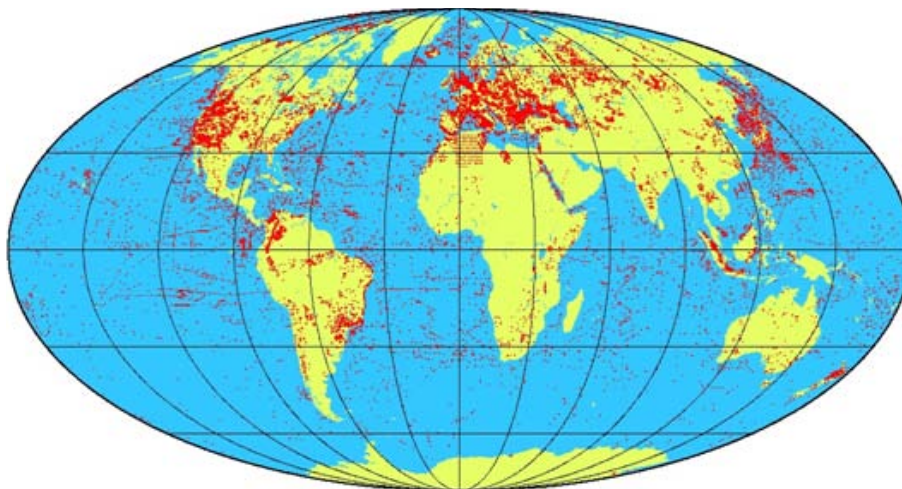
Interactive Discussion



**Table 1.** Summary of updated global heat flow data (derived from Vieira and Hamza, 2010).

	Regions	Number of Data	%
Continental	Africa	859	2.1
	Asia	4071	9.8
	Europe	5967	14.4
	Oceania	697	1.7
	North America	5008	12.1
	South America	3173	7.7
	Total Continents	19775	47.8
Oceanic	Atlantic	2400	5.9
	Indian	2066	4.7
	Pacific	10930	27.1
	Mediterranean	1682	4.2
	Inland seas and Gulfs	4533	11.2
	Total Oceans	21611	52.2
Global	Total	41386	100



**Global distribution of  
the lithosphere-  
asthenosphere**V. M. Hamza and  
F. P. Vieira

**Fig. 1.** Geographic distribution of heat flow measurements, as per the updated data base reported by Vieira and Hamza (2010).

Title Page

Abstract

Introduction

Conclusions

References

Tables

Figures

◀

▶

◀

▶

Back

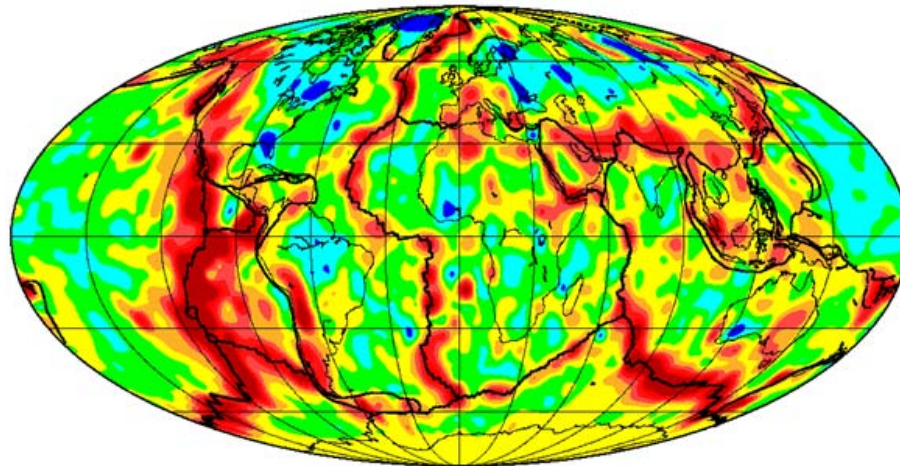
Close

Full Screen / Esc

Printer-friendly Version

Interactive Discussion



**Global distribution of  
the lithosphere-  
asthenosphere**V. M. Hamza and  
F. P. Vieira

**Fig. 2.** Global Heat Flow map derived from observational data (Vieira and Hamza, 2010) and estimated values based on heat flow – age relation (Hamza, 1967; Polyak and Smirnov, 1968; Hamza and Verma, 1969).

Title Page

Abstract

Introduction

Conclusions

References

Tables

Figures

◀

▶

◀

▶

Back

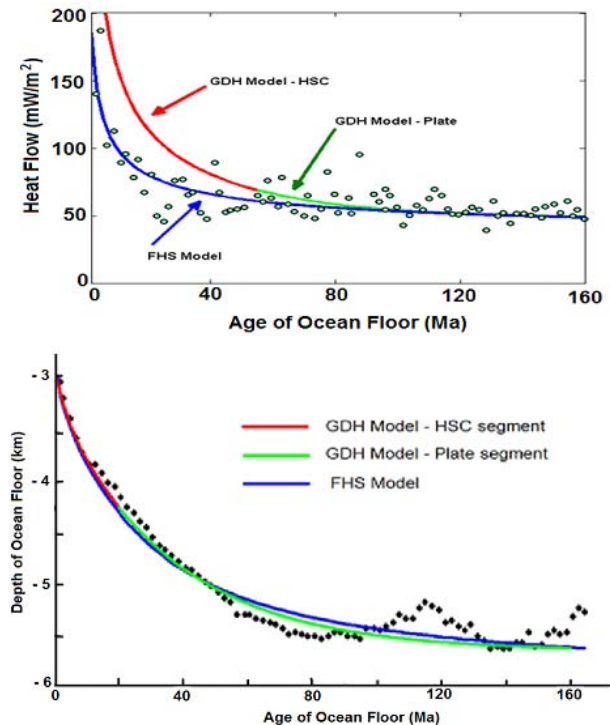
Close

Full Screen / Esc

Printer-friendly Version

Interactive Discussion



**Global distribution of the lithosphere-asthenosphere**V. M. Hamza and  
F. P. Vieira

**Fig. 3.** Comparison of fits to observational heat flow (upper panel) and bathymetry data (lower panel), by the GDH and FHS models. The GDH model fit being a hybrid version is composed of two segments, derived from HSC model (red curves) and Plate model (green curves).

Title Page

Abstract

Introduction

Conclusions

References

Tables

Figures

◀

▶

◀

▶

Back

Close

Full Screen / Esc

Printer-friendly Version

Interactive Discussion

**Global distribution of  
the lithosphere-  
asthenosphere**V. M. Hamza and  
F. P. Vieira

Title Page

Abstract

Introduction

Conclusions

References

Tables

Figures

◀

▶

◀

▶

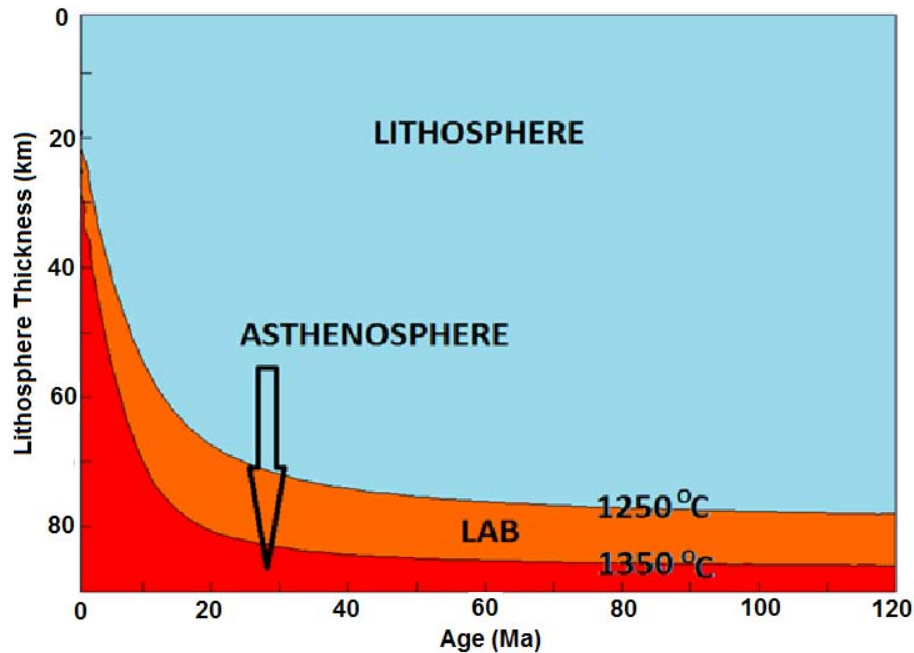
Back

Close

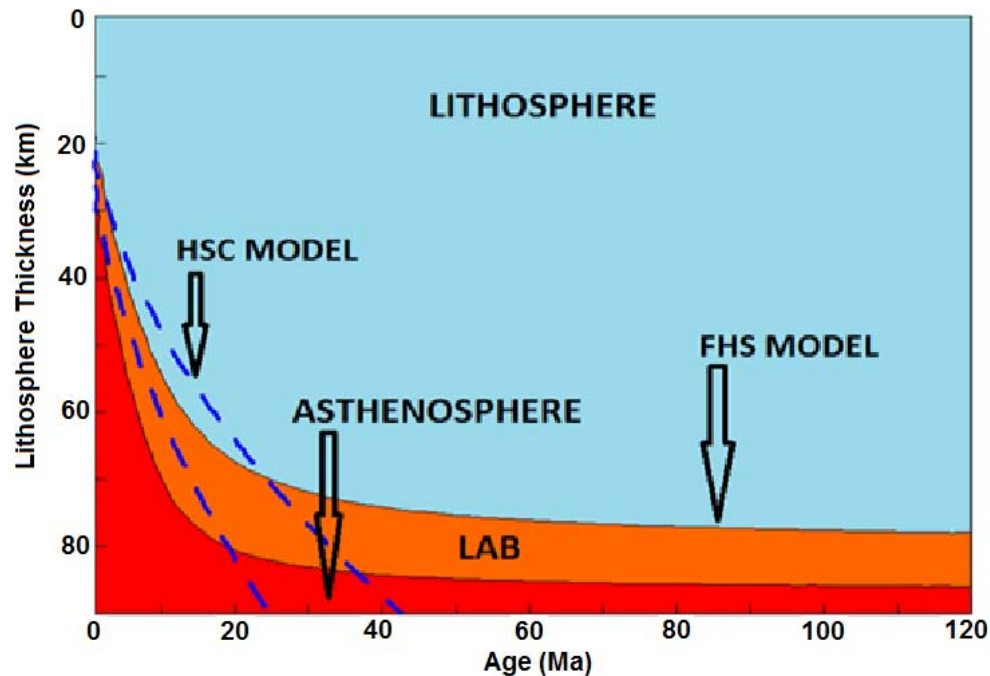
Full Screen / Esc

Printer-friendly Version

Interactive Discussion



**Fig. 4.** Variations in the thickness of the oceanic lithosphere with age, according to the Finite Half Space (FHS) model, for the case of basal geotherms of 1250°C and 1350°C.

**Global distribution of the lithosphere-asthenosphere**V. M. Hamza and  
F. P. Vieira

**Fig. 5.** Comparison of the variations in the thickness of the oceanic lithosphere with age, according to the Finite Half Space (FHS) and Half-Space Cooling (HSC) models. The dashed curves in this figure indicate depths of LAB in the HSC model.

Title Page

Abstract

Introduction

Conclusions

References

Tables

Figures

◀

▶

◀

▶

Back

Close

Full Screen / Esc

Printer-friendly Version

Interactive Discussion

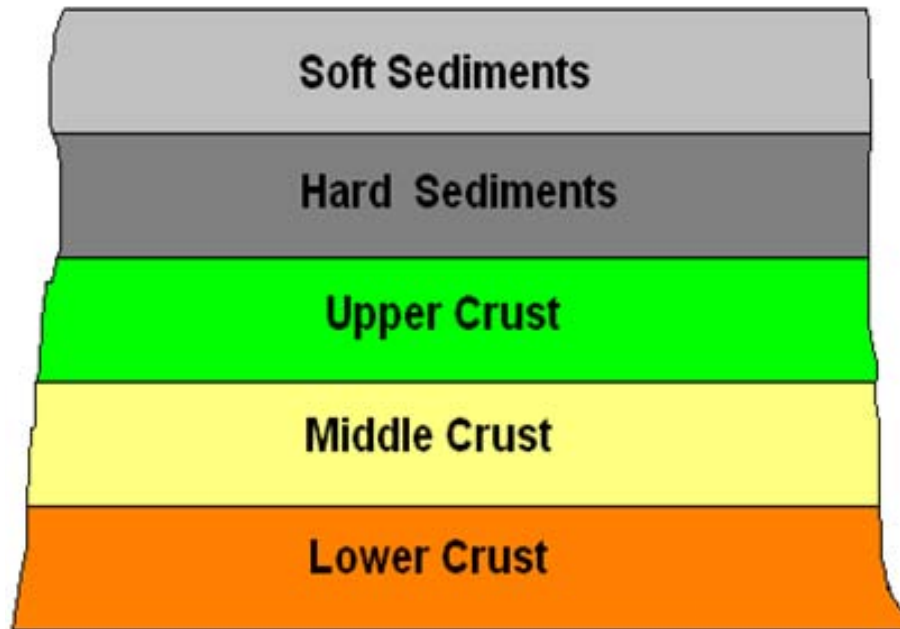


**Fig. 6.** Schematic representation of crustal structure proposed in the global crustal structure data set of Mooney et al. (1998).

**Global distribution of the lithosphere-asthenosphere**

V. M. Hamza and  
F. P. Vieira

Title Page

Abstract

Introduction

Conclusions

References

Tables

Figures

◀

▶

◀

▶

Back

Close

Full Screen / Esc

Printer-friendly Version

Interactive Discussion



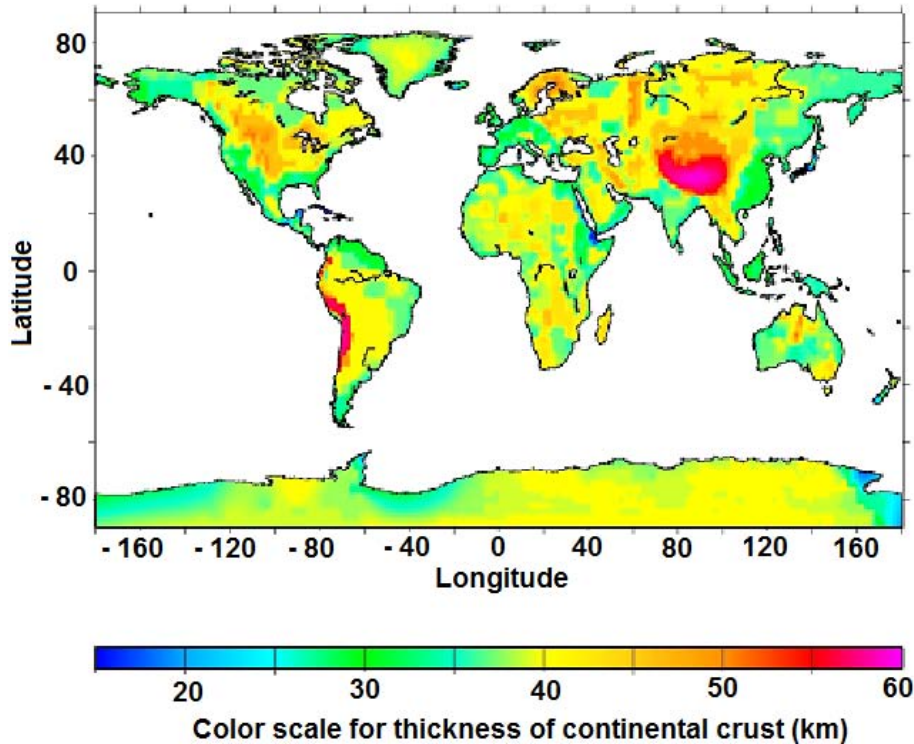


**Fig. 7.** Global distributions of the thickness of the continental crust, derived using data base of Mooney et al. (1998).

**Global distribution of the lithosphere-asthenosphere**

V. M. Hamza and  
F. P. Vieira

Title Page

Abstract Introduction

Conclusions References

Tables Figures

◀ ▶

◀ ▶

Back Close

Full Screen / Esc

Printer-friendly Version

Interactive Discussion



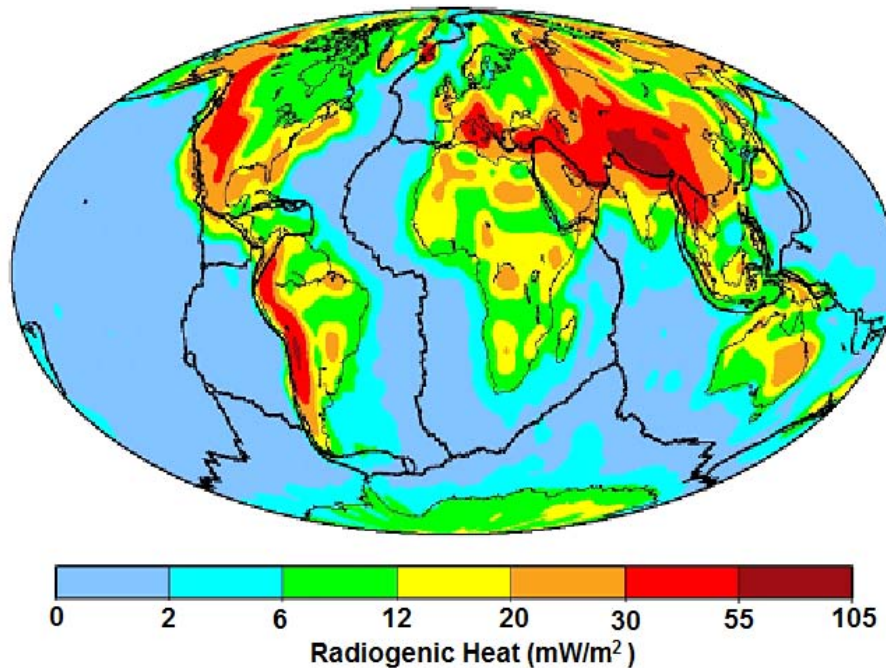


**Fig. 8.** Global map of heat flux produced by radiogenic elements in the Earth's crust, based on the crustal structure data set of Mooney et al. (1998) and the empirical relation between seismic velocity and heat production (Rybach and Buntebarth, 1984). Note the sharp contrast in heat production between continental and oceanic regions.

**Global distribution of the lithosphere-asthenosphere**

V. M. Hamza and  
F. P. Vieira

Title Page

Abstract Introduction

Conclusions References

Tables Figures

⏪ ⏩

◀ ▶

Back Close

Full Screen / Esc

Printer-friendly Version

Interactive Discussion



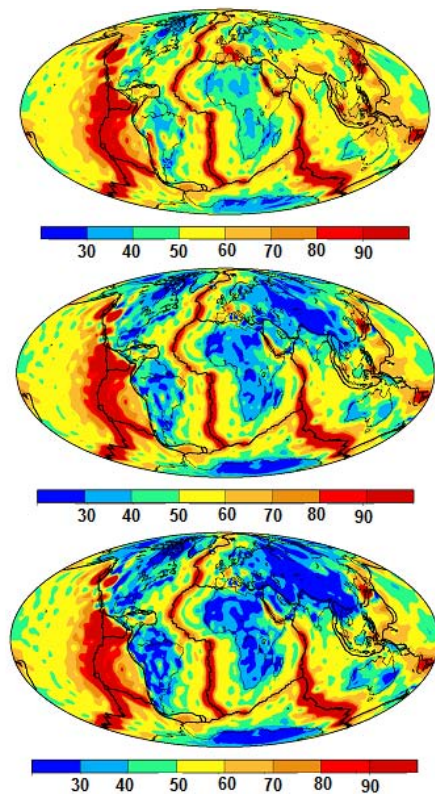


**Fig. 9.** Heat flow corrected for contributions of radiogenic heat at the base of sedimentary layers (upper panel), base of upper crust (middle panel) and base of lower crust (lower panel). Note that near surface heat flow (upper panel) provides very little clues as to the contrasts in the deep thermal structures of continental and oceanic regions. As the contributions of radiogenic heat of upper and lower crustal layers are progressively removed the differences in deep heat flux between these regions becomes evident (middle and lower panels).

**Global distribution of the lithosphere-asthenosphere**

V. M. Hamza and  
F. P. Vieira

Title Page

Abstract

Introduction

Conclusions

References

Tables

Figures

◀

▶

◀

▶

Back

Close

Full Screen / Esc

Printer-friendly Version

Interactive Discussion



**Global distribution of the lithosphere-asthenosphere**V. M. Hamza and  
F. P. Vieira

Title Page

Abstract

Introduction

Conclusions

References

Tables

Figures

◀

▶

◀

▶

Back

Close

Full Screen / Esc

Printer-friendly Version

Interactive Discussion

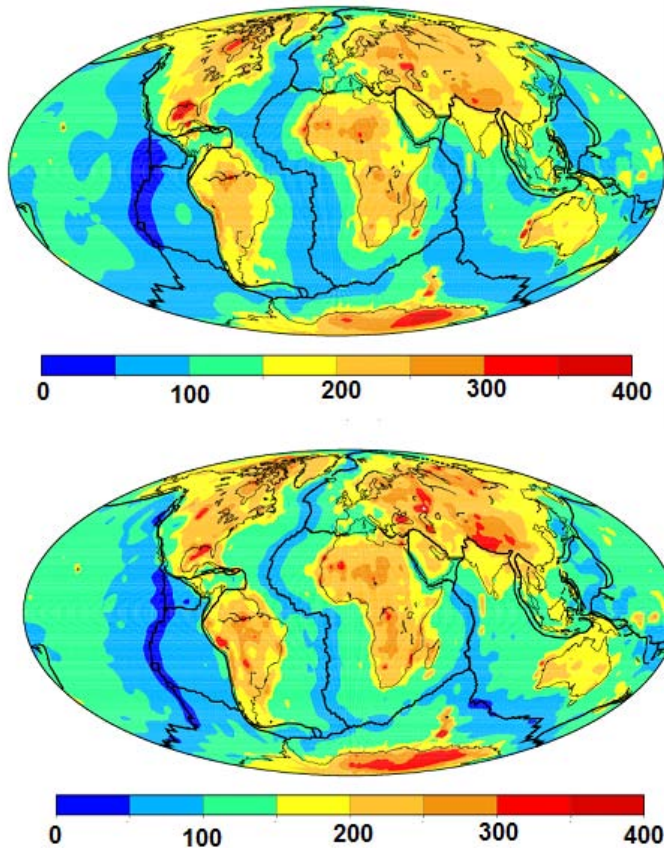


**Fig. 10.** Global distributions of depth to LAB in spherical harmonic representation (upper panel) and numerical interpolation methods (lower panel). Note that almost all of the continental areas are characterized by lithospheric thickness greater than 150 km.